



Development of Time Histories for IEEE693 Testing/Analysis and Their Validation by Numerical Simulations and Full-Scale Testing of Seismically Isolated Equipment

Shakhzod Takhirov⁽¹⁾, Eric Fujisaki⁽²⁾, Leon Kempner⁽³⁾, Michael Riley⁽⁴⁾

⁽¹⁾ Structures Laboratory – Eng. Manager, University of California at Berkeley, takhirov@berkeley.edu

⁽²⁾ Principal Engineer, Pacific Gas and Electric, emf1@pge.com

⁽³⁾ Principal Structural Engineer, Bonneville Power Administration, lkempnerjr@bpa.gov

⁽⁴⁾ Structural Engineer, Bonneville Power Administration, mjriley@bpa.gov

Abstract

The main objective of the paper is to address current developments for seismic qualification per IEEE Standard 693, Recommended Practice for Seismic Design of Substations. An extensive study conducted in 2003 on a set of strong motions to be used for IEEE 693 seismic qualifications resulted in the development of three-component time histories called TestQke4IEEE. Based on a detailed analysis, the best candidate was selected from a large set of the strong motions available at that time. TestQke4IEEE was developed from a historic record obtained during the 1995 Lander earthquake by matching its spectra in the time domain to the current IEEE693-2005 spectra. For more than a decade, the time histories have been successfully used for seismic qualification testing and analysis. Recent developments (e.g., M9 project for Cascadia subduction zone earthquakes) and records from recent earthquakes (e.g., the 2015 Nepal and the 2010 Chile earthquakes) clearly show a need to re-evaluate the time histories and the spectral demand specified by IEEE693-2005. It was clearly demonstrated that the strong motions in these regions can have long duration and high energy in a low frequency range. To address this issue, a set of strong motions, which is much larger than the one studied earlier, is investigated in the paper. This paper accounts for new time history records from the recent major earthquakes and assesses their effect on the spectral demand specified by IEEE693-2005. As one of the study's results, a set of time histories closely matching the IEEE693 spectra at 5% damping are developed which can be used for the seismic qualification of substation equipment without and with protection devices. A new annex that provides guidance for the use of seismic protective systems with substation equipment is one of many new changes proposed in the next version of the IEEE693 document. The paper describes the validation approach by means of numerical simulations and full-scale shaking table tests of a substation equipment with seismic isolation and damping devices. It is intended that future users of the new seismic protective systems annex will apply the time histories developed by this study.

Keywords: seismic qualification; numerical modeling and time history analysis; seismic isolation; damping devices; high-voltage substation equipment



1. Introduction

An extensive study conducted earlier on a number of strong motions [1] resulted in the development of three-component strong motion called TestQke4IEEEE. Based on a detailed analysis, the best candidate was selected from a large set of the strong motions. TestQke4IEEEE was developed from a historic record obtained during the 1995 Landers earthquake by matching its spectra to the current IEEE693-2005 [2] spectra. The spectral matching was performed in a time domain and, as a result, the TestQke4IEEEE spectra closely match the IEEE693-2005 [2] spectra at 2% of critical damping starting from about 0.35 Hz. For more than a decade, the strong motion have been successfully used for seismic qualification testing and analysis. This study was undertaken to address proposed changes in the IEEE693 document, account for the new strong motion records from the recent major earthquakes and assess their effect on spectral demand.

2. Development of IEEE693 Matched Strong Motions

The new version of IEEE693 document calls for input motions used for qualification to be matched to target spectra at 5% of critical damping and includes an annex focused on testing and/or analysis of seismically isolated equipment. The current three-component strong motion (TestQke4IEEEE) [1] was matched to IEEE693 spectra at 2% of critical damping and was not intended to be used for testing and/or analysis of isolated equipment with very low natural frequency. To address these two shortcomings (low frequency content and new damping value) a new extensive study on a large set of strong motions was conducted. This set is much larger than the one studied earlier [1] and includes major recent earthquakes. Due to limitations of the paper, only a summary of the study's major results is presented below.

2.1 Earthquake Records

The paper used PEER NGA-West2 ground motion database [3] that had been recently expanded significantly to account for the major recent earthquakes. The database was used in developing new Ground Motion Prediction Equations (GMPEs) [4]. GMPEs, or “attenuation” relationships, provide a means of predicting the level of ground shaking and its associated uncertainty at any given site or location, based on earthquake magnitude, source-to-site distance, local soil conditions, fault mechanism, etc. GMPEs are efficiently used to estimate ground motions for use in both deterministic and probabilistic seismic hazard analyses. The results of such hazard analyses are used for a wide range of applications such as: (1) site-specific seismic analysis and design of structures and facilities; (2) development of regional seismic hazard maps for use in building codes, financial estimation, etc.; and (3) social and financial loss estimation. Today, the most common Intensity Measures (IMs) used in GMPEs are peak ground motion values (e.g., peak ground acceleration, PGA; and peak ground velocity, PGV), and elastic spectral accelerations.

A major portion of the ground motion database used in this study is a subset of the PEER NGA-West2 ground motion database. The latter database includes over 21,000 three-component recordings from worldwide earthquakes with moment magnitudes ranging from 3.0 to 7.9. To meet the objectives of this paper, a selection of strong motions was based on many criteria, the majority of which were adapted from [4]. In addition, the records satisfying the following criteria were selected: (1) records having all three components; (2) moment magnitudes equal to 5.0 and higher; (3) the horizontal distance to rupture (R_{JB}) less than 50 km; (4) peak ground acceleration greater than 0.1g for all three components; and (5) maximum of 15 records from any event. The aftershocks were excluded. The records from more recent earthquakes were added from the Center for Engineering Strong Motion Data (CESMD) [5]. The resultant set consists of 410 records (each record has three components) collected during 85 events in total.

The plot in Fig. 1a shows a variation of the earthquake magnitude with R_{JB} (Joyner-Boore distance (km) - shortest horizontal distance from the recording site to the vertical projection of the rupture). This value is specified for each record in the PEER NGA-West2 ground motion database. For the records downloaded from CESMD database this distance is substituted by the epicentral distance. Because of the limited number of records collected in the immediate vicinity of the rupture, the resultant set has only a few records with R_{JB} less than 1 km. The variation of PGA of the records versus moment magnitude of the event is presented in Fig. 1b.



This plot also shows how many records are in close proximity to the rupture: cyan points are for the records with RJB less or equal to 2 km and blue points are for the records with RJB less or equal to 10 km.

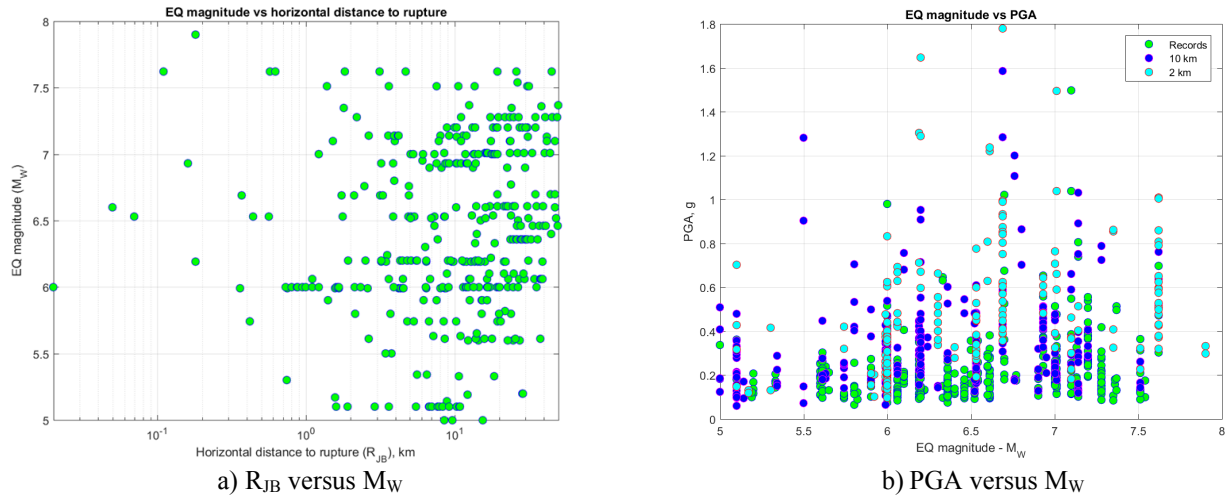


Fig. 1 – Variations of PGA and R_{JB} versus M_W for the selected records

Peak ground acceleration and peak ground velocities versus R_{JB} distance are presented in Fig. 2a and 2b, respectively.

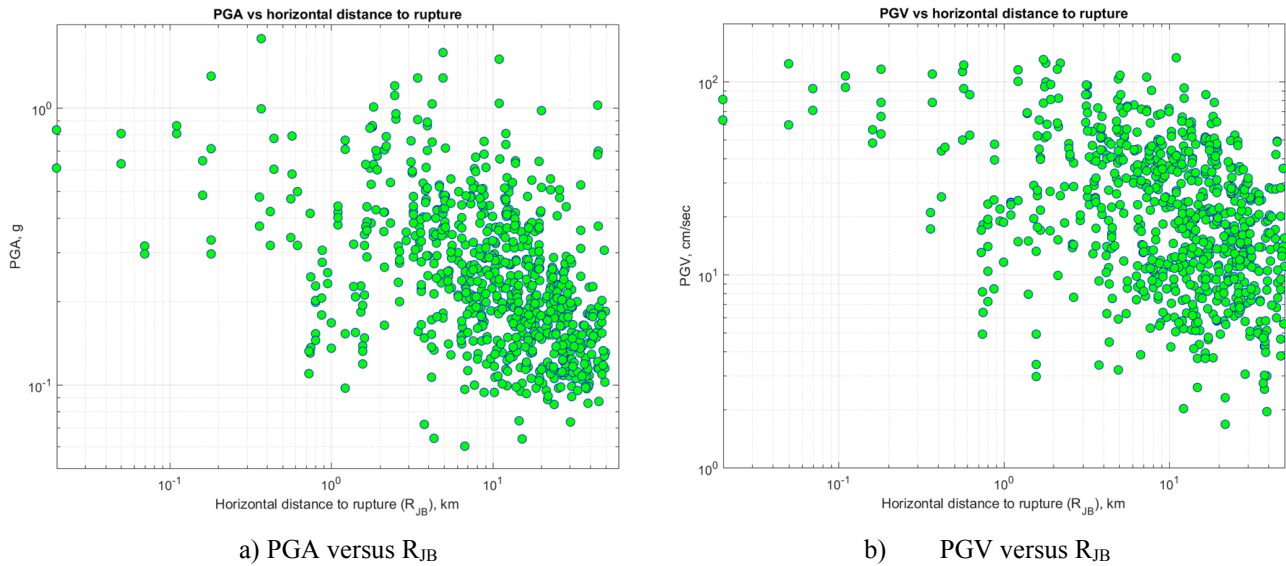
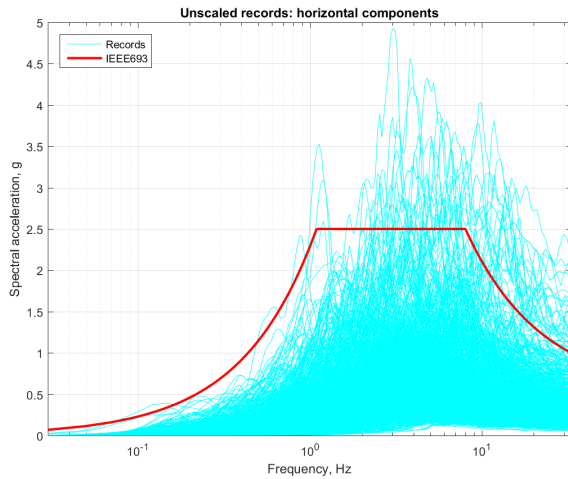


Fig. 2 – Peak ground values versus R_{JB}

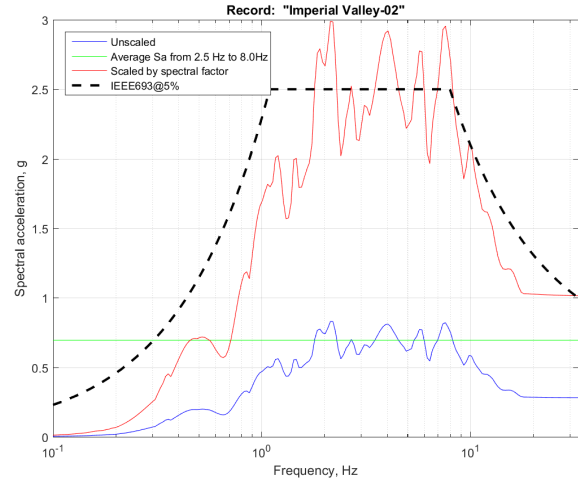
Spectral plots for all horizontal components of the set are presented in Fig. 3a. All spectra were computed at 5% of critical damping and no scaling factor was applied. As a reference, the IEEE693 High PL spectrum anchored at 1g is presented in red. In order to assess the suitability of candidate records to be used as seeds for matching to the IEEE 693 target spectra, various scaling schemes were considered. Among those, a scaling factor used in [6] was investigated in this study. The scaling factor was based on average spectral accelerations from 2.5 Hz to 8 Hz, S_a^{av} . The frequency range of 3 to 8.5 Hz was selected in [6] because it encompasses the highest portion of the horizontal acceleration response spectra of the near-source rock recordings from large magnitude earthquakes. For the purpose of this study, to remain within plateau frequencies of the IEEE693 spectra, this frequency range was slightly shifted and the scaling factor was based on average spectral accelerations from 2.5 Hz to 8 Hz. An example of this calculation for one of the time histories is presented in Fig. 3b.

As presented in 4a, the spectral mean from 2.5Hz to 8Hz has strong correlation with PGA and a slope of its linear approximation is less than the ratio of IEEE693 spectral plateau to PGA. The slope is close to 2, while the

IEEE693 ratio is 2.5. Mean spectra for all horizontal components of the set are presented in Fig. 4b. For the purpose of this paper, two possible normalization cases are shown: (1) based on normalization by PGA and (2) based on normalization by means of the average spectral acceleration from 2.5 Hz to 8.0 Hz. It worthy to note that both normalizations produce a mean spectrum that is very conservative and most likely does not reflect reality. It does not account for magnitude of the event, proximity to the source, type of the earthquake, soil conditions and so on. Therefore, the scaling factor of S_a^{av} is modified by means of attenuation relationships derived earlier and provided in [6].

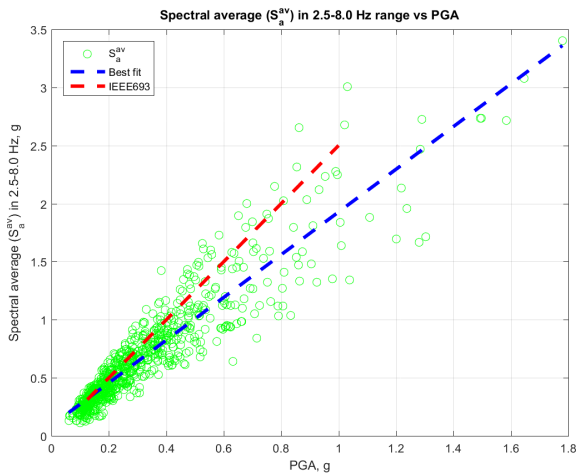


a) IEEE693 High PL spectrum versus spectra of unscaled motions

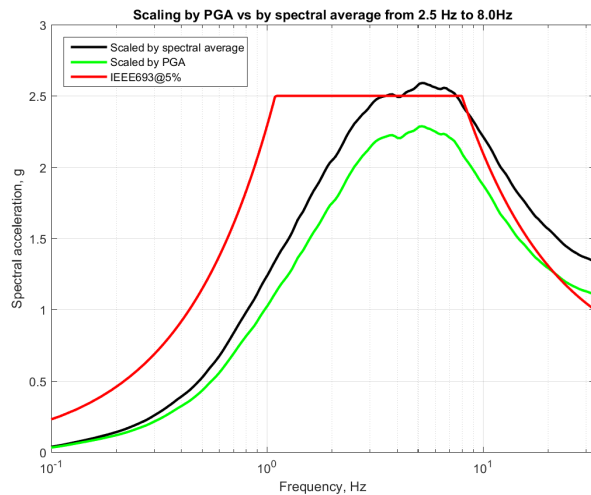


b) Example of scaling (mean spectral acceleration from 2.5 Hz to 8.0 Hz is set at IEEE693 plateau)

Fig. 3 – Response spectra for the set



a) Correlation between mean spectral acceleration, S_a^{av} , and PGA



b) Mean of spectra normalized by S_a^{av} and PGA

Fig. 4 – Response spectra for normalized set

2.2 Parameters of Time Histories

The study of the entire set was based on the analysis of several parameters commonly used to evaluate strong motions. The parameters and their descriptions are provided below.

Peak ground acceleration. One of the most commonly used parameters to describe the strong motion record is peak ground acceleration (PGA). The PGA is calculated as a maximum of absolute value of the acceleration.



The value of PGA can be presented as a number with dimensions of the acceleration in any particular measuring system or as a fraction of g , where g is an acceleration due to gravity, that is 386.4 in./sec^2 (9.81 m/sec^2).

Peak ground velocity. Peak ground velocity (PGV) is another important parameter commonly used to characterize a strong motion record. A strong motion record usually represents an acceleration time history recorded at a particular location; therefore, the determination of the velocity time history involves some data manipulation. The acceleration time history has to be numerically integrated over the time, and the absolute maximum of the delivered velocity time history yields the PGV. Depending on the selected measuring system, the PGV is presented in in./sec (m/sec).

Cumulative energy. For engineering purposes, the cumulative energy of a strong motion record, CE , is defined as the area under the squared acceleration record, and represents a measure of intensity of the record:

$$CE = \int_0^t a(\tau)^2 d\tau,$$

where $a(t)$ is a time history of the acceleration and t is a length (measured in seconds) of the strong motion record. Depending on the selected measuring system, the cumulative energy can be presented in $\text{in.}^2/\text{sec}^3$ (m^2/sec^3) or simply in $g^2 \text{ sec}$.

Root mean square acceleration. The computed cumulative energy can be used in calculating the parameter of a strong motion record known as the “root mean square” (RMS) acceleration, A_{RMS} , commonly used to characterize amplitude of the accelerogram:

$$A_{RMS} = \sqrt{CE/t}$$

In contrast to the peak ground acceleration (PGA), the RMS acceleration takes into account the complete ground motion time history and is a factored mean amplitude for the entire accelerogram. The RMS acceleration is usually presented in fractions of g .

Durations based on CE definition. A method to calculate a duration of a strong motion record based on using the cumulative energy was proposed by Dobry, et al [7]. The method defines the duration in seconds, D_{5-95} , as the time interval required to accumulate between 5% and 95% of the accelerogram’s maximum cumulative energy. In addition, another duration parameter is commonly used to characterize a time history. This duration, D_{25-75} , is defined as the time interval required to accumulate between 25%–75% of the maximum cumulative energy. Based on its definition it is measured in seconds. In one of the recent publications [8], another duration parameter was introduced that can be suitable for studying the impact of ground motion duration in structural collapse risk assessment. This duration, D_{5-75} , is measured in seconds and is defined as the time interval required to accumulate between 5%–75% of the maximum cumulative energy.

Duration based on IEEE693 definition. In the IEEE693-2005 document [2] the bracketed duration is defined as the time interval between the first and the last occurrences of accelerations equal to or larger than 25% of the maximum value of the acceleration.

Cycle counts in time history. In order to classify the strong motion in terms of fatigue analysis, a cycle counting procedure is used. The procedure is based on the commonly used ASTM procedure, called the “simplified rain flow cycle counting procedure” [9]. The cycle counting procedure yields a histogram of cycle counts for the magnitude range of the cycles. The procedure counts the cycles of the accelerogram in order to deliver a number of cycles in the excitation’s acceleration imposed on equipment.

Cycle counts in a single-degree-of-freedom (SDOF) system subjected to the time history. The parameter [1] represents the number of high cycles in the acceleration response of the SDOF system plotted against the natural frequency of the system and calculated for a fixed damping value. Only cycles with relatively high magnitude are included in the high cycle count: the study uses a threshold of 70% of the maximum magnitude. The study uses a 5% damping value and calculates the number of high cycles only for frequencies of a strong part of the IEEE693 spectrum that covers frequencies from 0.78–11.78 Hz.

Parameters based on best fit to the IEEE693 spectrum. Two more parameters were introduced to characterize proximity of the spectral shape of each time history to that of the IEEE693 spectrum. They were based on a cumulative distance, D_{SA} , between each spectral acceleration, S_i , factored by scaling factor K_S , and the IEEE693 spectral point, S_i^{IEEE} , at the same frequency, which is defined as follows:

$$D_{SA} = \text{sqrt}(\sum(K_S S_i - S_i^{IEEE})^2).$$

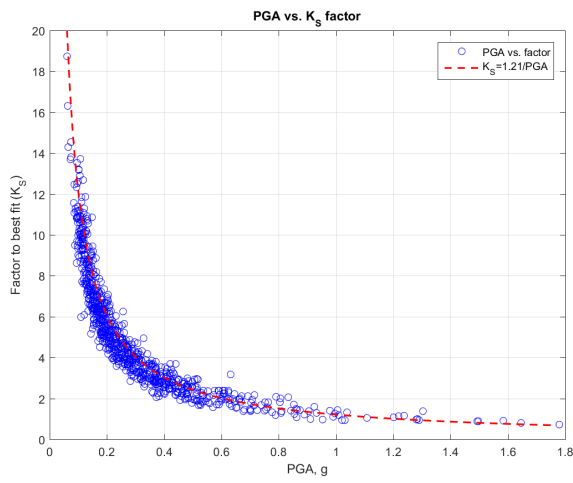
This cumulative distance will be at its minimum when;

$$dD_{SA}/dK_S = 0.$$

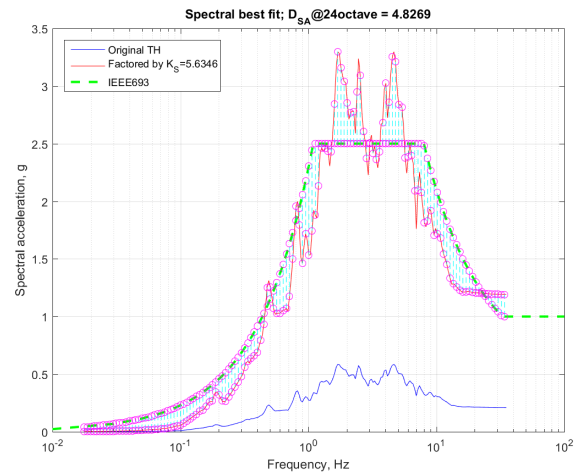
The latter equation is satisfied when:

$$K_S = \sum(S_i * S_i^{IEEE}) / \sum(S_i^2).$$

This scaling factor was computed for each horizontal component of the set as presented in Fig. 5a. The plot clearly shows that a larger factor is needed for smaller PGA values and the K_S versus PGA relationship can be closely approximated as $K_S = 1.21/PGA$. An example of scaling to best fit the IEEE693 spectrum and values of K_S and D_{SA} for sample time history is presented in Fig. 5b. There is very weak correlation between PGA and D_{SA} as presented in Fig. 6a. Since both K_S and S_a^{av} are correlated to PGA, they have a strong correlation in the log-log scale as presented in Fig. 6b.

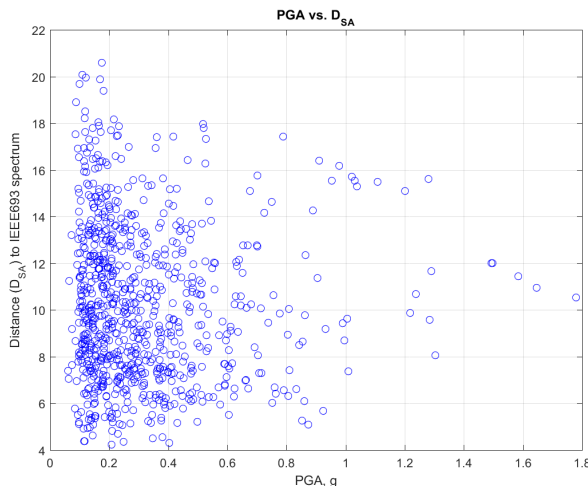


a) Relationship between K_S and PGA

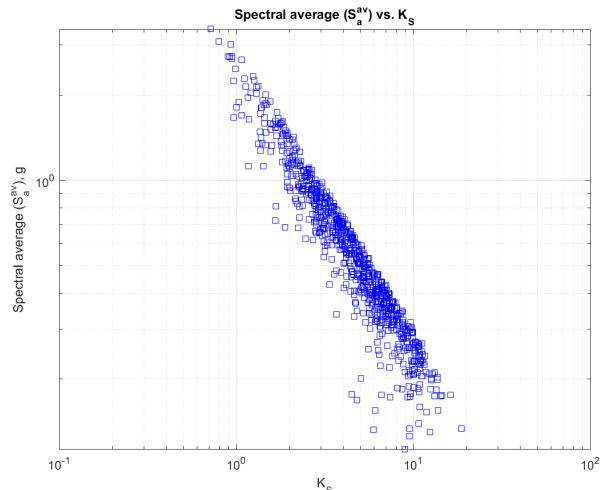


b) Example of scaling to best fit IEEE693 and D_{SA} computation

Fig. 5 – Results for best fit factor and cumulative distance to IEEE693 spectrum



a) D_{SA} versus PGA

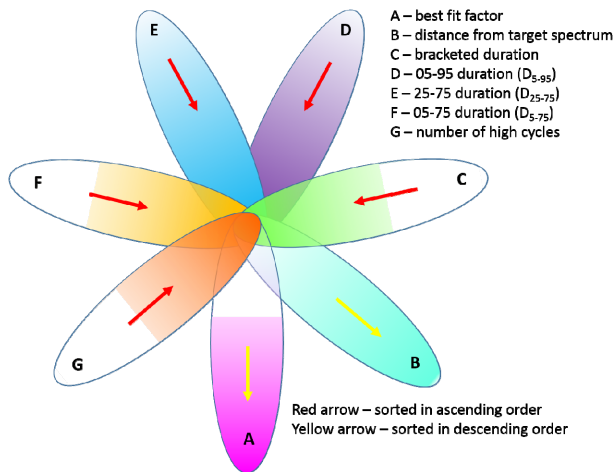


b) correlation between S_a^{av} and K_S

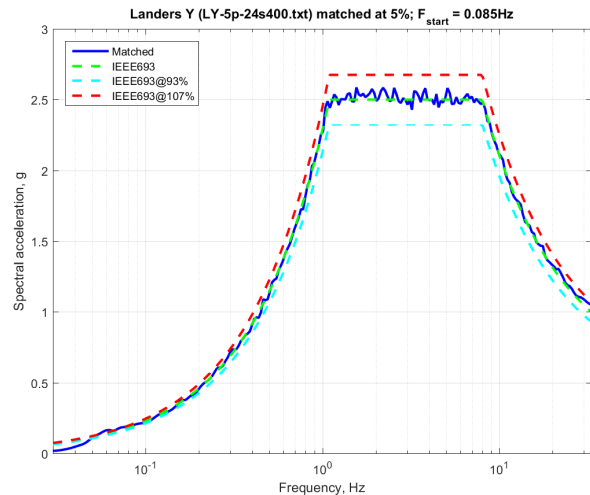
Fig. 6 – Cumulative distance to IEEE693 spectrum

2.2 Selection of Seed Motions

The entire set of time histories was studied by analyzing all parameters defined in the previous section of the paper. Selection criteria for seed motions were based on the following. First, the strong motions with the smallest scaling factor were identified. This approach was undertaken to minimize an excessive scaling needed for large best fit factors. Second, the strong motions with the smallest cumulative distance to the IEE693 spectrum were identified. Smaller cumulative distance means that the spectral shape of a time history is ‘naturally’ closer to that of IEE693 spectrum. Third, the strong motions with longer durations in several definitions were identified. This approach was undertaken to make sure that the seed strong motions are long enough to satisfy the duration requirement of the IEE693-2005 document [2]. Fourth, the strong motions with larger cycle counts were identified. The seed motions were selected as an intersection of all these subsets as presented in Fig. 7a. As a result, four seed motions were selected as presented in Table 1. Three strong motions will become a set recommended by the IEE693 document and one of the four will remain optional. As an example, one of the motions from Table 1 that was matched in time domain to the IEE693 spectrum is presented in Fig. 7b. The matching starts from 0.085 Hz and spectral peaks and valleys are well within $\pm 7\%$ tolerance zone. A matching procedure developed by Norm Abrahamson [10] was utilized to perform the matching in time domain.



a) Schematic diagram of selection criteria for seed motions



b) Sample seed motion matched to IEE693 spectrum

Fig. 7 – Selection criteria for seed strong motions and a sample seed motion matched to IEE693

Table 1 – Seed motions selected from parameter analysis

| Seed No | PEER ID | Earthquake | Bracketed duration, sec |
|---------|------------|--------------------------|-------------------------|
| 1 | PEER-00864 | Landers, USA | 28.40 |
| 2 | PEER-01513 | Chi-Chi, Taiwan | 26.20 |
| 3 | PEER-06952 | Darfield, New Zealand | 25.01 |
| 4 | PEER-05823 | El Mayor-Cucapah, Mexico | 32.75 |

3. Validation of New Annex on Seismically Isolated Equipment

The main objectives of the second part of the research summarized herein are: (1) conduct shaking table tests of seismically isolated equipment to test the developed time histories and (2) validate the approach of the new Annex W proposed for the next version of IEEE695 document. Annex W specifies qualification procedures for seismically isolated equipment.

3.1 Shaking Table Tests

A new set of the strong motions matching the IEEE693 spectra have much more demanding peak table velocity and peak table displacement for qualifying seismic protective devices. Therefore, this time history set cannot be tested, including the peak velocity and displacement demands, on existing 6DOF shaking tables in the United States due to their somewhat limited displacement capacity. The new time histories will be filtered for qualifying substation equipment not using protective devices. To address the issue of using the non-filtered time histories, a new shaking table with long-stroke and high-velocity capabilities was developed at the University of California, Berkeley. It is a uniaxial shaking table with stroke capacity of ± 34 in and peak velocity of about 80 in/sec as presented in Fig. 8a. As shown in Fig. 8b, sample equipment isolated by wire ropes is tested as a representative example.

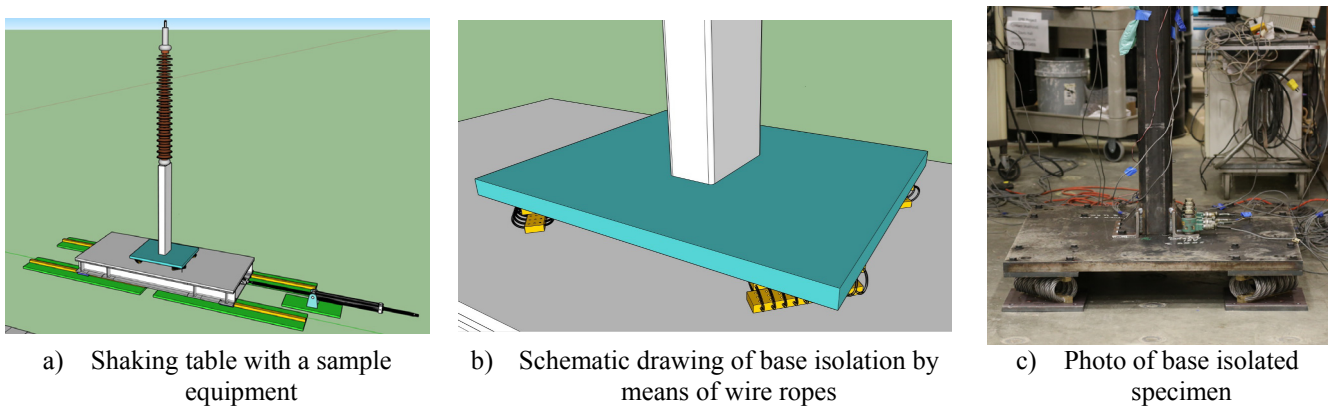


Fig. 8 – Shaking table test of seismically isolated equipment

Manufacturers of wire ropes provide detailed drawings similar to the one depicted in Fig. 9a. In addition to that, they supply a set of plots and specifications based on the testing of one or many wire ropes as presented in Fig. 9b. Obviously these data are not sufficient to model the complex nonlinear performance of the wire ropes. For example, the plots in Fig. 9b do not provide any information about (1) variability from sample to sample, (2) cyclic performance of wire ropes, (3) performance under combined shear and axial load application, and (4) rate dependency (if any). Therefore, Annex W specifies additional information and testing that is needed to be conducted for proper characterization and subsequent modelling of the wire ropes.

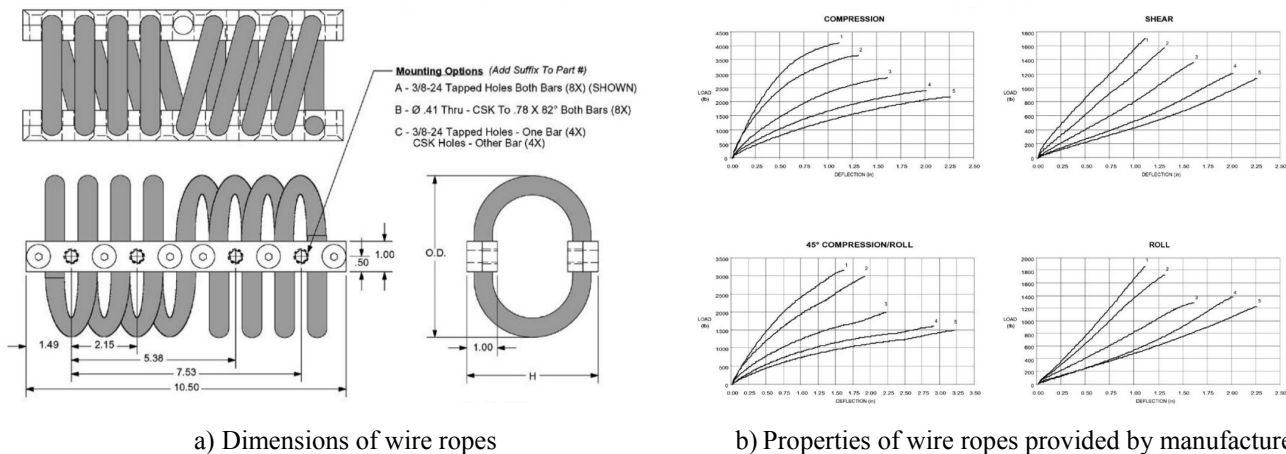


Fig. 9 – Typical information usually supplied by manufacturer

To address these shortcomings, an extensive component testing is conducted in the course of this study. The test setup is presented in Fig. 10.

Annex W specifies a set of requirements for component testing of seismic protective devices. These component tests were conducted in this study. Two types of testing are identified: (1) prototype and (2) production, See Figure 11. For prototype tests, the following sequence of tests need to be performed: (1) five fully-reversed cycles of loading at each of the following increments of the performance level displacement, D_{PL} , — 0.25, 0.5 and 1.0 (2) five fully-reversed cycles of loading at 1.1 times D_{PL} , (3) fifteen fully-reversed cycles of loading at 0.75 times D_{PL} , Figure 11a. For production tests, as a minimum, the test program comprises three fully-reversed cycles of loading times the performance level displacement, D_{PL} , see Figure 11b . If the force-deflection properties of the seismic protective device are not dependent on rate of loading, the production tests need not be dynamic. For each cycle of each test, the force-deflection and hysteretic behavior of the test specimen was recorded.

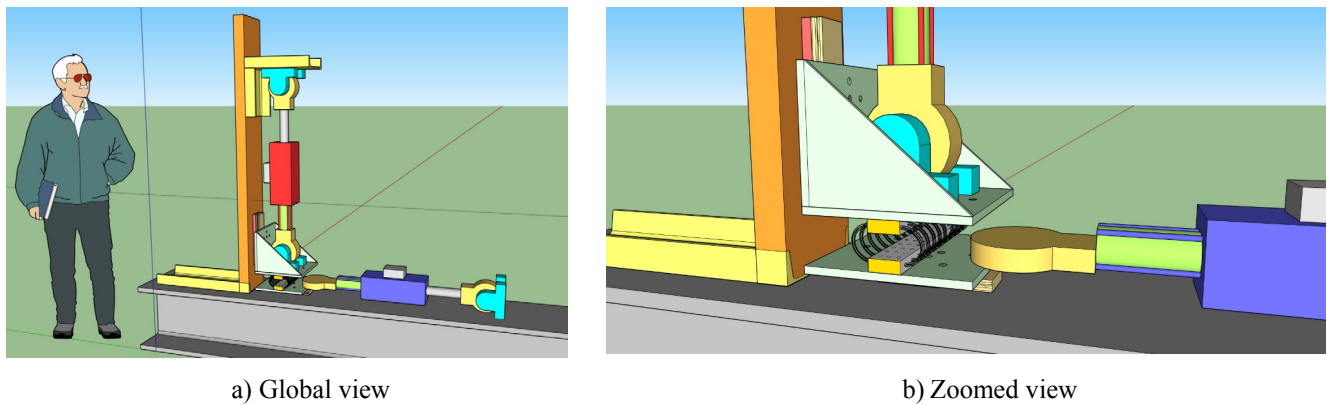


Fig. 10 – Schematic views of component testing setup

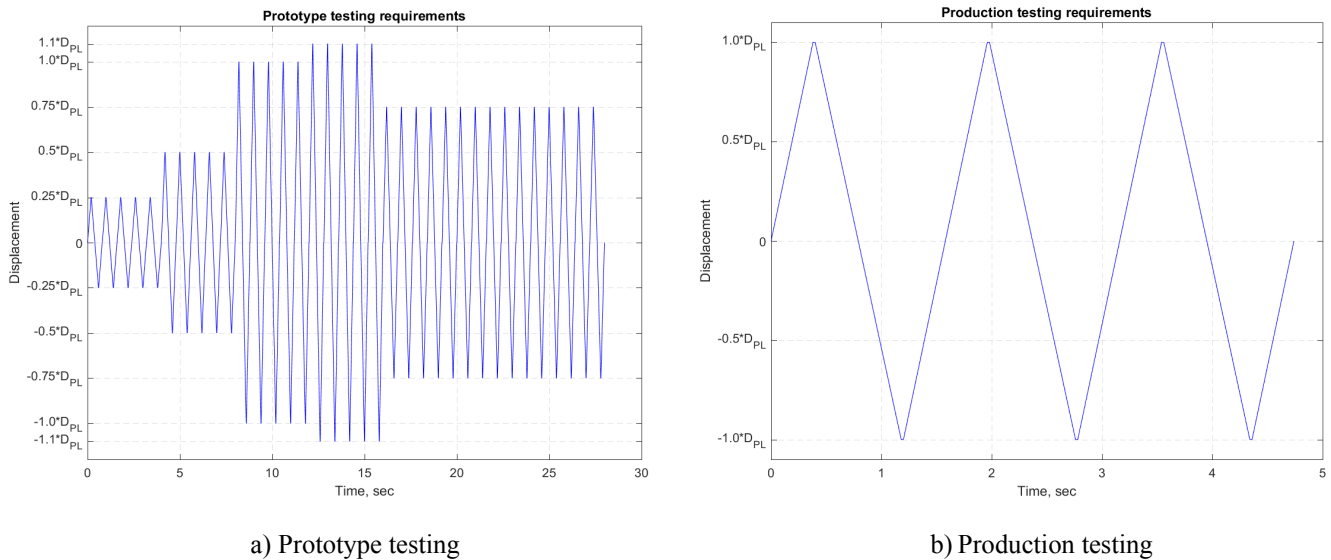


Fig. 11 – Component testing requirements from Annex W

The test protocol presented in Fig. 11 was applied to investigate performance of the wire ropes. Due size limitations of the paper, only some tests are discussed herein. Those results of the component testing program are presented in Fig. 12. The left plot presents compression force versus vertical displacement diagram of the wire rope in cyclic loading compared to monotonic loading data provided by the manufacturer. The positive force corresponds to compression and the negative force corresponds to tension. This plot shows that the vertical stiffness of the wire is dependent on the amount of vertical load. Therefore, the performance of the wire rope in shear (the so-called ‘roll’ testing) was studied for two different vertical pre-loading conditions: (1) no pre-load

and (2) with a pre-load of 1400 lbs. The vertical load was kept constant during the test. The test results show that the roll stiffness of the wire rope is dependent on the pre-load as presented in the right plot of Fig. 12. The images of the wire rope taken during the roll tests are presented in Fig. 13.

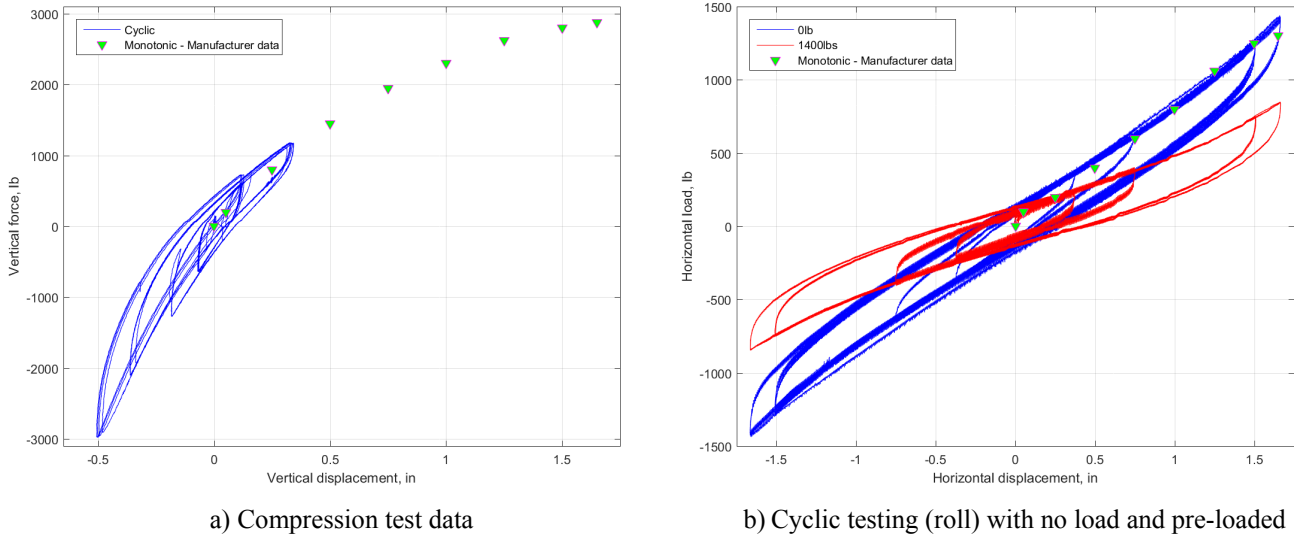


Fig. 12 – Results of component tests compared to manufacturer data

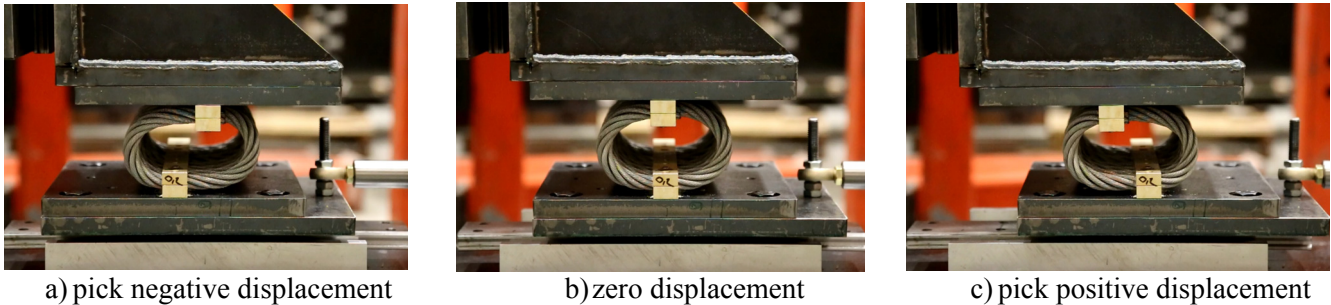


Fig. 13 – Images of wire rope in roll tests (vertical load remained constant)

In addition to the component testing, some variability in a test specimen is incorporated into the test program. The test specimen consists of a support structure and the equipment. The support structure is constructed from a HSS with well separated natural frequencies in both horizontal directions. Two insulators with the same voltage rating of 230-kV but different material (porcelain and polymer) are used in the study. Two sets of four wire ropes with two different stiffnesses are available for the shaking table testing. The list of test specimens is provided in Table 2.

Table 2 – List of test specimens for shaking table tests

| Specimen No | Insulator | Number of wire ropes | Fixed or Isolated |
|-------------|-----------|----------------------|-------------------|
| 1 | Polymer | 0 | Fixed |
| 2 | Porcelain | 0 | Fixed |
| 3 | Polymer | 4 stiff WRs | Isolated |
| 4 | Porcelain | 4 stiff WRs | Isolated |
| 5 | Polymer | 4 soft WRs | Isolated |
| 6 | Porcelain | 4 soft WRs | Isolated |



Based on the results of component testing detailed numerical models of the seismically protected equipment are to be generated. They will be used in a blind prediction of its seismic performance. The predictions will be compared to the full-scale tests on the shaking table. The testing phase is currently underway and results of the modelling phase are not presented in the paper.

4. Conclusions

An extensive study on a large set of strong motions including major recent earthquake has been conducted. A set of seed motions was selected based on the analysis of the major parameters of the strong motions. The seed motions were matched to the IEEE693 spectra at 5% of critical damping with very tight tolerance. The spectral matching was conducted in the time domain. The developed strong motions will be tested on a uniaxial shaking table. A set of seismically isolated equipment will be analyzed and tested to validate the approach specified in Annex W of the proposed next version of IEEE693.

5. Acknowledgements

Special thanks are due to the staff of the Structure Laboratory at the University of California, Berkeley. The successful completion of the testing phase of the project would not be possible without this technical support. Technical help by Mr. Henry Teng (CEE, UC Berkeley) on modelling and testing is greatly appreciated.

6. Copyrights

16WCEE-IAEE 2016 reserves the copyright for the published proceedings. Authors will have the right to use content of the published paper in part or in full for their own work. Authors who use previously published data and illustrations must acknowledge the source in the figure captions.

7. References

- [1] Takhirov S., Fenves G., Fujisaki E., and Clyde D. 2005. 'Ground Motions for Earthquake Simulator Qualification of Electrical Equipment', Pacific Earthquake Engineering Research Center, University of California at Berkeley, PEER 2004/07, January 2005.
- [2] IEEE, 2005. IEEE STANDARD 693-2005 - IEEE Recommended Practice for Seismic Design of Substations.
- [3] <http://ngawest2.berkeley.edu/site>
- [4] Campbell, K.W. and Y. Bozorgnia, "NGA-West2 ground motion model for the average horizontal components of PGA, PGV, and 5%-damped linear acceleration response spectra," *Journal of Earthquake Spectra*, August 2014, Vol. 30, pp. 1087-1115, doi: 10.1193/072113EQS209M.
- [5] <http://strongmotioncenter.org/>
- [6] PG&E (1988). Long Term Seismic Program (LTSP) for Diablo Canyon Power Plant. *Technical Report*.
- [7] Dobry, R., Idriss, I.M., and Ng, E. 1978. Duration Characteristics of Horizontal Components of Strong Motion Earthquake Records. *Bulletin of the Seismological Society of America*, 68(5): 1487-1520.
- [8] Reagan Chandramohan, Jack W. Baker, and Gregory G. Deierlein (2016): Impact of hazard-consistent ground motion duration in structural collapse risk assessment, *Earthquake Engineering & Structural Dynamics*, 45, 1357–1379.
- [9] ASTM, 1986. ASTM E1049 - 85. (Reapproved 1997) 'Standard Practices for Cycle Counting in Fatigue Analysis'. American Society for Testing and Materials, *Annual Book of ASTM Standards, Section 3: Metals Test Methods and Analytical Procedures*, Vol. 03.01-Metals-Mechanical Testing; Elevated and Low-Temperature Tests, ASTM, Philadelphia, 1986, pp. 836-848.
- [10] Abrahamson, N. 1996. Non-Stationary Response Spectral Matching. Non-published paper.